October 1976 LRP 120/76

EXPERIMENTS ON PLASMA INTERACTIONS WITH POWERFUL RF DISCHARGES

A. Lietti

Centre de Recherches en Physique des Plasmas
ECOLE POLYTECHNIQUE FEDERALE DE LAUSANNE

October 1976 LRP 120/76

EXPERIMENTS ON PLASMA INTERACTIONS WITH POWERFUL RF DISCHARGES

A. Lietti

ABSTRACT

Linear discharges in a steady axial magnetic field are produced in hydrogen plasmas by means of unconventional line generators. The current non decaying pulses range from 1 to 50 kA at a frequency of 3 MHz. The penetration of the azimuthal oscillating field is observed, and the influence of limiters is investigated. A critical current is found, and this result is compared with previous theory.

Anomalous skin depth results from analysis of the complex wave vector, which shows energy exchanges with the plasma, in addition to the normal joule heating. Decreasing conductivity at low densities indicates possible turbulent behaviour.

An interesting feature of the discharges in the highest power range is the excitation of magnetosonic compressional waves at the second harmonic of the axial current with typical resonance effect. This quadratic interaction, not observed before, is explained with a simple model considering the pressure gradient at the plasma boundary.

1. INTRODUCTION AND PREVIOUS WORK

Interest in plasma interaction with rf fields has been motivated mainly, in thermonuclear research, by dynamical stabilization and heating schemes. Experiments requiring very high rf power have been, however, generally limited by the available equipment.

Consider linear discharges with $I = I_z \cos\omega t$ in a steady axial magnetic field. The product ωI_z is a crucial parameter for the feasability of the experiment, if power availability and insulation problems are considered.

Early work along this experimental line has been reported by BOBYREV (1966) and GORDIENKO et al. (1968). With typical values of $\omega I_z = 10^{10}$ [DUBOVOI et al. (1970)] dynamical stabilization as well as anomalous heating has been observed. In these previous experiments attention was paid to the penetration of the azimuthal magnetic field. Insulating diaphragms have been reported to improve such penetration. From that time, however, insulating limiters at higher intensity have been rarely used and positive [HOFFMANN et al. (1972)] as well negative [GRUBER (1972)] results have been reported for different experimental conditions. Experiments with decaying pulses (capacitor discharges) are reported by GRIBBLE (1969) and BEREZIN (1972). The current was increased and the frequency decreased. The ωI_z product, however, was increased by a factor ten ($\omega I_z = 10^{11}$). The result of this previous work can be summarized as follows.

The experimental proof of the dynamic stabilization of the low modes has been generally recognized. Anomalous heating rates have been generally observed, suggesting turbulent behaviour. The problem of the radial distribution of the energy remains however still unresolved, because the current carrying layer generally develops near the wall and the efficiency of insulating diaphragms at large current is controversial. This paper reports experiments performed with a special technical facility which improves ωI_z by a factor ten ($\omega I_z = 10^{12}$). Moreover the rf pulse is not decaying and allows investigation in an unexplored area.

2. APPARATUS AND DIAGNOSTICS

A schematic diagram of the experimental installation is shown in Fig. 1.

2.1 The Discharge Tube and the Auxiliary Circuitry

The discharge tube of 15 cm diameter and 114 cm length is evacuated by a turbomolecular pump (base pressure 10^{-7} Torr). The tube is equipped with cylindrical end electrodes and is situated within a coil which produces an axial magnetic field. The field can be varied from 0.1 to 1 T and remains constant during the discharge. The experiments are carried on with hydrogen gas, whose filling pressure ranges from 1 to 100 mTorr.

To ensure breakdown at low pressure and partial preionization, an E x B preliminary discharge is produced by means of an HF prepulse (6 MHz) applied symmetrically to two coaxial ausiliary end electrodes. The preionization can be improved by a supplementary unidirectional 2 μs pulse.

2.2 Radio Frequency Generators and Matching Circuits

The 3 MHz main discharge is produced by a special line generator. To improve the efficiency of the energy transfer from the rf generator to the experiment, a resonant circuit allows the plasma column to resonate with two capacitors stacks symmetrically arranged at the ends of the tube. In fact the plasma column with the axial current return paths, located around the tube, can be considered as a section of transmission line whose impedance is mainly inductive at the working frequency. The correct impedance matching with the generator is obtained by a proper choice of the length of the cables, connecting the generator with the experiment. Line pulse generator techniques and rf plasma matching methods have been reported by LIETTI (1968, 1969).

2.3 The rf Main Discharge

In this experiment the intensity of the 3 MHz non decaying discharge pulse can be varied from 1 to 50 kA, the duration from 5 to 15 μs. The reproducibility of the pulse depends on the experimental conditions, it generally improves with increasing filling pressure of the hydrogen gas. At a given time the variation of the current amplitude from one shot to another goes from $\pm$ 15% to $\pm$ 5% for filling pressures going from 3 to 100 mTorr. To compensate for these variations, unless otherwise specified, the measured data which will be reported in this paper have been averaged over five shots.

2.4 Diagnostic Methods

The diagnostic techniques include internal magnetic probes, external current and voltage probes, diamagnetic loops, spectroscopic observation, interferometry and fast photography.

Magnetic probes can be inserted radially in the central midplane of the tube and allow measurement to be made of the field profile. This way, when a skinned state is reached, the local position of the plasma column can be determined, while its average position, as well as the incoming energy, can be deduced from analysis of the voltage-current function. Simultaneous measurement of the mean electron density (axial interferometry), average transverse energy (diamagnetic loop signals) and Doppler broadening (spectral analysis in the center midplane) allow an estimation of n, T_e and T_i.

3. EXPERIMENTAL RESULTS

Three different topics of this experiment will be separately presented and discussed: the influence of limiters, the analysis of the skin layer, and the magnetosonic resonance effect. Unless otherwise specified MKS units are used.

3.1 The Influence of Limiters

The efficiency of the limiters to control the rf axial current flow and to improve the penetration of the oscillating magnetic field was tested as follows. Two quartz diaphragms with a 4 cm hole were symmetrically placed 74 cm apart in the discharge tube, and discharges with different current intensities and gas filling pressure were performed. The end electrodes had the same diameter as the diaphragms hole. Only HF pre-ionization was used. The initial plasma density ranged from 10^{18} to 10^{19} m^{-3} according to the gas filling pressure.

The axial steady field was 0.4 T.

In no more than one microsecond a definite skinned state was observed, the skin depth δ being generally lower than one centimeter. Since $\delta \ll R$ (tube radius), a plasma column "radius" r can be considered, which indicates the location of the current flow. Time evolution of r, averaged over the tube length, is shown in Fig. 2 at different discharge currents (filling pressure 5 mTorr). Fig. 3 shows the dependence of r on the current at different filling pressures. The existence of a critical current I_{cr} is evident. When $I_z > I_{cr}$ the limiters do not control the current any more. The fast expansion of the plasma column with a current beyond the critical limit has also been observed by image converter axial framing photography (Fig. 4). Note that the expansion is symmetrical, no m = 1 instability mode is observed, as occurs in unidirectional discharges, beyond the Kruskal-Shafranov limit. The view that the expansion does not originate from this instability mode is further supported by the observation that the plasma column expends faster with increasing density, as Fig. 3 shows. Moreover the growth rate of the instability has been estimated to be smaller than the rate of change ω of the oscillating current. As a consequence, dynamical stabilization would be expected. This feature has been considered by GORDIENKO et al. (1968).

A more recent study, however, considers the propagation of Alfvèn wave in the dilute plasma outside the central column [JONES et al. (1974)] . A critical parameter $\varepsilon = \omega L/2V$ is considered (L is the axial length between

the limiters, V is the Alfvèn speed) and it is shown that the limiters are effective only when $\varepsilon < 1$.

In this experiment the plasma is only partly ionized at the beginning of the main discharge, and the electron density increases with time. Fig. 5 shows ε and r as a function of time in a critical 4 kA discharge. An increase of the expansion growth rate is observed when $\varepsilon \to 1$.

Note that the Alfvèn speed has been deduced from the estimated density and the filling gas mass. This way impurities can somehow introduce an error. Even if this argument is considered, we conclude that the theory gives a possible explanation of the experimental observation.

3.2 The Skin Layer

The investigations about the skin layer were performed under the following experimental conditions : axial magnetic field 0.4 T, maximum I_z current 20 kA, preionizing d.c. pulse 3 kA, 2 μs, electrodes diameter 12 cm. No diaphragms were used. The skin depth was measured at the midplane of the discharge tube, and the values were averaged in the interval 1-5 μs after the beginning of the discharge.

We investigate the penetration of the azimuthal magnetic field produced by the oscillating axial I_z current. The skin depth being small compared to the radius of the plasma column, a plane geometry is considered. In this coordinate system, the y direction corresponds with the radius, the positive sense of the y axis being directed towards the center of the tube. Consider the wave equation :

$$B_x = B \exp\left[i(ky-\omega t)\right] \tag{1}$$

Quite generally, we can write :

$$-ik = \frac{1}{\alpha} + i\frac{1}{\beta} = \frac{\sqrt{2}}{\delta} \exp\left[i\left(\frac{\pi}{4} + \frac{\theta}{2}\right)\right] \tag{2}$$

where α, β are real quantities.

When the field penetrates into a conducting medium, where the current is simply proportional to the electric field, equation (2) reduces to the usual skin effect formula : $\alpha = \beta = \delta_o$; $\theta = 0$. We refer to this situation as "normal skin". In this experiment δ and θ have been deduced from the observation of phase and amplitude of the magnetic field as a function of radius. The result of average measurements in various discharges at different filling pressure of the hydrogen gas is given below :

mTorr	H_2	5	10	20	60	100
δ	cm	0.52	0.30	0.20	0.27	0.30
θ	rad	-0.22	-0.63	0.56	0.64	-0.62

Since the measurements give $\theta \neq 0$, the field penetration deviates from the "normal" one, showing a somewhat "anomalous" skin effect.

In Appendix 1 a theoretical exploration has been made to understand the physical meaning of this deviation.

As a result, some evidence has been found that $\theta \neq 0$ simply means that not all the energy entering in the medium is dissipated in joule heating of the skin layer. The total power delivered to the medium is given by

$$W = W_o \frac{\delta}{\delta_o} \sqrt{1 + \sin \theta} \qquad (3)$$

where W_o is the power dissipated in joule heating in the normal case. $\theta \neq 0$ means additional power exchanges to or from the medium. Plasma motion and wave coupling can eventually contribute to these extra exchanges. We suggest wave coupling to be more likely to occur in this experiment, since no gross plasma motion was detected in the time interval of the skin measurement. Further analysis in the matter requires additional information about the plasma state and therefore we will not go any further in this investigation now. We simply note that, from the measured values of θ, at least 75% of the exchanged power is dissipated in joule heating of the skin layer.

Another point, however, is worth being considered. The electrical conductivity σ can be deduced from the skin depth measurements; and compared with the classical conductivity σ_{cl}, as results from calculation on the ground of the estimated electron temperature. Since the temperature, which reaches about $4 \cdot 10^5$ K at the lowest density, decreases with increasing density, the ..... (see page 8)

classical conductivity decreases. Fig. 6 shows σ and σ_{cl} as a function of density. An estimation of the velocities ratio v_{drift}/v_{sound} has been also indicated, and strongly suggests that the decrease in conductivity at low densities, which results from the measurements, can be produced by ion-acoustic instabilities. This possibility was discussed by SKARSGARD (1973).

3.3 Magnetosonic Resonance

A B_z field, which oscillates at the second harmonic of the axial current frequency was detected in the high current, low pressure discharges. Fig. 7 shows a signal recorded on the axis of the tube in a typical discharge. The current amplitude was I_z = 50 kA, the steady axial field B_0 = 0.4 T, the electron density n = 10^{20} m^{-3}.

Fig. 8 shows the radial profile of B_z having the maximum amplitude on the axis, which is typical of compressional magnetosonic waves in cylindrical geometry. These waves are well-known, see for example WOODS (1962), and CANTIENI and SCHNEIDER (1963). The waves are generally excited by a coil, wounded around the tube, which produces a B_z oscillating field. The excitation by means of an axial current, with frequency doubling, suggests a quadratic effect, which, as far as we know, has not been reported until now. We assume that in previous experiments the excitation threshold was not reached.

The coupling of these waves with the current simply originates from the pressure gradient at the boundary layer, produced by the skinned B_θ field. The calculation is carried out in Appendix 2 with a simple two fluids MHD model.

It results that the oscillating B_z fields can be expressed as follows:

$$B_z(r) = \frac{J_0[K(r+\delta)}{J_0(KR)} F \frac{\mu_0^{\frac{3}{2}} I_z^2}{8 \delta \omega \sqrt{\varrho}} \frac{1}{(\pi R)^2} \qquad (4)$$

where now the frequency of I_z is $\frac{1}{2}\omega$, δ is the skin depth and ϱ is the ion density.

The damping function F can be deduced from the transport coefficients of the plasma, as shown in Appendix 2. A calculation with classical coefficients, however, results in values of B_z higher than the experimental ones. Additional damping, therefore, must be considered. In this experiment, a satisfactory agreement between the expression (4) and the measurements can be obtained assuming $F/J_0(KR) = \alpha$ (experimental damping constant). In this manner, $B_z(r=0)$ was calculated as a function of density and current. Fig. 9 compares the result with the experiment.

Finally, Fig. 10 shows measurements of B_z as a function of the steady magnetic field B_0 at various densities. Typical resonance effect results at densities which corresponds to minimums of the Bessel function $J_0(KR)$, in agreement with equation (4). Since $Im(K) \ll Re(K)$ this occurs when $KR \approx 2.4$.

CONCLUSION

The investigation of rf discharges one order of magnitude larger than in previous experiments allows a number of interesting observations. This powerful interaction presents many aspects concerning the plasma dynamics, heating and wave coupling. The investigation about the limiters shows that their utility depends on the intensity of the discharges. This conclusion accounts for previous controversial results. The penetration of the azimuthal field depends on the skin effect. Anomalous heating has been observed, but the energy is deposited mainly in the outer region of the plasma. More interesting is the penetration of the B_z field due to magnetosonic resonance. A quadratic coupling of waves and current has been observed for the first time.

ACKNOWLEDGMENT

The author is pleased to acknowledge M.H. Skarsgard for suggesting the experiment. He would like to thank K. Appert, J.-M. Peiry, F. Troyon and J. Vaclavik for useful discussions and R. Means for reading the manuscript. He is indebted to L. Bighel for helpful advice in the spectroscopic observations, to A. Heym for making available the interferometer, to C. Rizzo and to the technical personnel of the C.R.P.P. for general assistance with the experiment.

This work was supported by the "Fonds National Suisse de la Recherche Scientifique".

APPENDIX 1

SKIN EFFECT CALCULATION

In the plane model considered here, the wave vector (2) is directed toward the Y axis. The linear surface current intensity is given by

$$\underset{z}{I}(t) = I \exp(-i\omega t) = \int_0^\infty \underset{z}{j}(y,t)\, dy \tag{5}$$

Taking in account the Maxwell equations

$$\frac{\partial E_z}{\partial y} = -\frac{\partial B_x}{\partial t} \; ; \qquad \frac{\partial B_x}{\partial y} = -\mu_0 \underset{z}{j} \tag{6}$$

and the boundary condition (5), the penetration of fields and current can be described by the following relations

$$B_x(y,t) = -\mu_0 I \exp -\left[\frac{y}{\alpha} + i\left(\frac{y}{\beta} + \omega t\right)\right] \tag{7}$$

$$E_z(y,t) = \frac{\mu_0 \omega \delta}{\sqrt{2}} I \exp -\left[\frac{y}{\alpha} + i\left(\frac{y}{\beta} - \frac{\pi}{4} + \frac{\theta}{2} + \omega t\right)\right] \tag{8}$$

$$\underset{z}{j}(y,t) = \frac{\sqrt{2}}{\delta} I \exp -\left[\frac{y}{\alpha} + i\left(\frac{y}{\beta} - \frac{\pi}{4} - \frac{\theta}{2} + \omega t\right)\right] \tag{9}$$

When $\theta = 0$ this system gives the normal skin effect relations. The total average power transferred to a unit surface of the medium is given by the Poynting vector

$$W = \frac{1}{\mu_0} \left\langle \underset{z}{E}(0,t) \; B_x(0,t) \right\rangle_{av} \tag{10}$$

or by the volume integral of the j·E product

$$W = \frac{1}{T}\int_0^T dt \int_0^\infty j_z E_z dy = \frac{1}{T}\int_0^\infty dy \int_0^T j_z E_z dt \tag{11}$$

where $T = \frac{2\pi}{\omega}$. Both calculations give

$$W = \frac{1}{2} R I^2 \tag{12}$$

where R is the surface resistance

$$R = \frac{\omega \mu_0 \delta}{2} \sqrt{1+\sin\theta} = \frac{\omega \mu_0 \delta}{2} \frac{\delta}{\beta} \tag{13}$$

The expressions giving W and R differ from the one's occuring in the normal skin effect by the factor:

$$\frac{\delta}{\delta_0} \sqrt{1+\sin\theta} = \frac{\delta^2}{\beta \delta_0} = \frac{R}{R_0} = \frac{W}{W_0} \tag{14}$$

More information about the energy flow requires a relation connecting current and fields. For the normal skin effect, (θ=0) an elementary Ohm's law applies:

$$j_z = \sigma E_z \tag{15}$$

A simple example of a situation where $\theta \neq 0$, can be given if we consider plasma motion in the y direction. Ohm's law becomes now

$$j_z = \sigma (E_z - v_y B_x) \tag{16}$$

and the total power

$$W = W_j + W_m \tag{17}$$

where W_j is the joule heating

$$W_j = \frac{1}{2}\sqrt{\frac{\mu_0 \omega}{2\sigma}}\ \frac{1}{\sqrt{\cos\theta}}\ I^2 \tag{18a}$$

and W_m the mechanical power

$$W_m = \frac{1}{2}\sqrt{\frac{\mu_0 \omega}{2\sigma}}\ \sqrt{\sin\theta}\ I^2 \tag{18b}$$

comparing now W ($v \neq 0$) and W_0 ($v = 0$) we found

$$\frac{W}{W_0} = \frac{1}{\sqrt{\cos\theta}} + \sqrt{\sin\theta} = \frac{\delta}{\beta}\sqrt{\frac{\alpha}{\beta}} \tag{19}$$

$\frac{W}{W_0} > 1$ when $v > 0$ (compression)

$\frac{W}{W_e} < 1$ when $v < 0$ (expansion)

From (14) and (19) we have : $\frac{\delta}{\delta_0} = \sqrt{\frac{\alpha}{\beta}}$ (20)

APPENDIX 2

WAVE COUPLING CALCULATION

We consider a plane model with a steady magnetic field B_0 in the z direction. The motion of ion and electron fluids is described by the equations of momentum, state (adiabatic condition), continuity, together with Maxwell's equations. Frictional, but not viscous terms are retained.

Since we are interested in magnetosonic plane waves propagating in the y direction, only the vector components relevant for these waves are considered. We obtain the following linearized set of equations:

$$m_i n_o \frac{\partial v_{iy}}{\partial t} = -e n_o v_{ix} B_o - \frac{\partial p_i}{\partial y} - m_i n_o \nu_{in} v_{iy} - m_e n_o \nu_{ei} (v_{iy} - v_{ey}) \tag{21}$$

$$m_e n_o \frac{\partial v_{ey}}{\partial t} = e n_o v_{ex} B_o - \frac{\partial p_e}{\partial y} - m_e n_o \nu_{en} v_{ey} - m_e n_o \nu_{ei} (v_{ey} - v_{iy}) \tag{22}$$

$$m_i n_o \frac{\partial v_{ix}}{\partial t} = e n_o (E + v_{iy} B_o) - m_i n_o \nu_{in} v_{ix} - m_e n_o \nu_{ei} (v_{ix} - v_{ex}) \tag{23}$$

$$m_e n_o \frac{\partial v_{ex}}{\partial t} = -e n_o (E + v_{ey} B_o) - m_e n_o \nu_{en} v_{ex} - m_e n_o \nu_{ei} (v_{ex} - v_{ix}) \tag{24}$$

$$\frac{\partial E}{\partial y} - \frac{\partial B}{\partial t} = 0 \tag{25}$$

$$\frac{\partial p_i}{\partial y} = \gamma_i k T_i \frac{\partial n_{1i}}{\partial y} \tag{26}$$

$$\frac{\partial p_e}{\partial y} = \gamma_e k T_e \frac{\partial n_{1e}}{\partial y} \tag{27}$$

$$\frac{\partial n_{1i}}{\partial t} + n_0 \frac{\partial v_{iy}}{\partial y} = 0 \tag{28}$$

$$\frac{\partial n_{1e}}{\partial t} + n_0 \frac{\partial v_{ey}}{\partial y} = 0 \tag{29}$$

E and B represent the x and z components of the oscillating electric and magnetic field. The particle density is $n_{i,e} = n_0 + n_{1-i,e}$; $\frac{n_1}{n_0} \ll 1$; $\frac{B}{B_0} \ll 1$.

We consider wave solutions: $e^{i(ky-\omega t)}$; $\frac{\partial}{\partial y} = ik$; $\frac{\partial}{\partial t} = -i\omega$; from continuity equations results

$$\frac{n_{1,i}}{n_0} = \frac{v_{iy}}{V} \quad ; \qquad \frac{n_{1,e}}{n_0} = \frac{v_{ey}}{V} \tag{30}$$

where $V = \frac{\omega}{k}$. Equations (26) and (27) become now

$$\frac{\partial p_i}{\partial y} = i k \, n_{1i} \gamma_i k T_i \; ; \quad \frac{\partial p_e}{\partial y} = i k \, n_{1e} \gamma_e k T_e \tag{31}$$

We introduce the following notations:

$$\omega_{in} = \frac{\nu_{in}}{\omega} \; ; \quad \omega_{ei} = \frac{\nu_{ei}}{\omega} \; ; \quad \frac{m_e}{m_i} = \mu \tag{32}$$

$$\Omega = \frac{\omega}{\omega_{ci}} \; ; \quad (\gamma_{i,e} k T_{i,e}) / (m_{i,e} V^2) = \tau_{i,e}$$

and substitute in Eq.(21-25). We obtain a linear system of equation, whose unknown are the velocities:

$$v_1 = v_{ix}\,; \qquad v_2 = v_{ex}\,; \qquad v_3 = v_{iy}\,; \qquad v_4 = v_{ey} \tag{33}$$

$$u_j = \frac{v_j}{V\frac{B}{B_0}} \quad (j = 1-4)\,; \qquad [a]\,[u] = \begin{bmatrix} 1 \\ 1 \\ 0 \\ 0 \end{bmatrix}$$

The elements of the matrix $[a]$ are:

(18 a.)

$$a_{11} = \Omega\left(-\omega_{in} - \mu\omega_{ei} + i\right); \qquad a_{12} = \Omega\mu\omega_{ei}\,; \qquad a_{13} = 1\,; \qquad a_1$$

$$a_{21} = -\Omega\mu\omega_{ei}\,; \qquad a_{22} = \Omega\mu\left(\omega_{en} + \omega_{ei} - i\right); \qquad a_{23} = 0\,; \qquad a_2 \tag{18 b}$$

$$a_{31} = -1\,; \quad a_{32} = 0\,; \quad a_{33} = \Omega\left[-\omega_{in} - \mu\omega_{ei} + i\left(1 - \tau_i\right)\right]; \quad a_{34} = \Omega\mu$$

$$a_{41} = 0\,; \quad a_{42} = 1\,; \quad a_{43} = \Omega\mu\omega_{ei}\,; \quad a_{44} = \mu\Omega\left[\left(-\omega_{en} - \omega_{ei}\right) + i\right. \tag{19}$$

The solution of (34) gives the velocities and substituting in Eqs.21 and 22 we obtain a non-dimensional function F:

$$F^{-1} = \frac{B_0}{\omega\rho V B}\,\frac{\partial\left(p_i + p_e\right)}{\partial y} = \Omega^{-1}\left(u_{ex} - u_{ix}\right) - \mu\left(\omega_{en} - i\right)u_{ey} - \left(\omega_{in} - i\right)u_{iy} \tag{35}$$

Consider now an equilibrium situation, where the plasma is contained in the $y > 0$ space by a magnetic field gradient, which results from an oscillating current, flowing on the y = 0 plane in the z direction. The linear current density

$$I_l = \hat{I}\cos\tfrac{1}{2}\omega t \tag{36}$$

produces the magnetic field

$$B_x(y) = \frac{1}{2}\mu_0 I_\ell e^{-\frac{y}{\delta}} \tag{37}$$

The skin depth δ develops a magnetic pressure gradient

$$\frac{\partial p_M}{\partial y} = -\frac{\mu_0}{8\delta}\hat{I}^2 \cos\omega t\, e^{-\frac{2y}{\delta}} \tag{38}$$

At the boundary, y = 0, the amplitudes of the magnetic pressure and the plasma pressure balance so that

$$\frac{\partial p_i}{\partial y} + \frac{\partial p_e}{\partial y} + \frac{\partial p_M}{\partial y} = 0 \tag{39}$$

and substituting in Eq.(35) we found the oscillating B_z field at the boundary:

$$B_z = F\,\frac{\mu_0 B_0 I^2}{8\delta\omega\rho V} \tag{40}$$

where $\rho = nm_i$ is the ion density.

The solution (40) can be used as a boundary condition of the plasma column of radius R. This can be allowed in this experiment because $\delta \ll R$.

The extension to the cylindrical case is then straight forward, when the well-known solution for the fundamental mode of magnetosonic wave is considered.

We obtain

$$B_z(r) = \frac{J_0(Kr)}{J_0(KR)}\,F\,\frac{\mu_0^{\frac{3}{2}} I_z^2}{8\delta\omega\sqrt{\rho}}\,\frac{1}{(\pi R)^2} \tag{41}$$

where I_z is now the total axial current. Note that the dependence on B_0 disappears by introducing the approximate relation $V \cong \frac{B_0}{\sqrt{\mu_0\rho}}$.

REFERENCES

BEREZIN A.B. et al. (1972) Soviet Phys. JTP, 17, 750.

BOBYREV N.A. (1966) Soviet Phys.JTP, 11, 316.

CANTIENI E. and SCHNEIDER H. (1963) Helv.Phys.Acta, 36, 993.

DUBOVOI L.V. et al. (1970) Soviet Phys. JETP, 31, 8.

GORDIENKO V.P. et al. (1968) Soviet Phys. JETP, 27, 185.

GRIBBLE R.F. et al. (1969) 3rd European Conference on Controlled Fusion and Plasma Physics, p. 79, Utrecht, Holland.

GRUBER O. (1972) Z.Physik, 251, 333.

HOFMANN F. et al. (1972) 5th European Conference on Controlled Fusion and Plasma Physics, p. 49, Grenoble, France.

LIETTI A. (1968) Rev.Scient.Instrum. 39, 900.

LIETTI A. (1969) Rev.Scient.Instrum. 40, 473.

SKARSGARD H.M. (1973) Laboratory Report LRP 64/73 - Ecole Polytechnique Fédérale, CRPP, Lausanne, Switzerland.

WOODS L.C. (1962) J.Fluid Mech. 13, 570.

JONES I.R., PEIRY J.M. and TROYON F. (1974) Nuclear Fusion, 14, 497.

ILLUSTRATION LEGENDS

Figure 1: Schematic diagram of the experimental installation

Figure 2: The evolution of the plasma column radius at different discharge currents

Figure 3: Dependence of the plasma column radius on the current at different filling pressures

Figure 4: a) Discharge current
b) Exposure time
c) Framing photographs

Figure 5: r(t) and $\mathcal{E}$(t) in a critical 4 kA discharge at 5 mTorr filling pressure

Figure 6: Measured and classical conductivity (σ_m, σ_{cl}) as a function of density. The ratio v_{drift}/v_{sound} is also indicated

Figure 7: Upper trace I_z current
Lower trace B_z field on the axis of the tube
B_0= 0.4 T, n = 10^{20} m^{-3}

Figure 8: Radial profil of $B_z \sim j$; I_z= 50 kA, B_0= 0.4 T, n = 10^{20} m^{-3}

Figure 9: The points show values of $B_z(r = 0)$ at the resonance. The lines correspond to Eq.(4) assuming $F/J_0(KR) = \alpha = 4.5$

Figure 10: Resonance effect in the 50 kA discharges

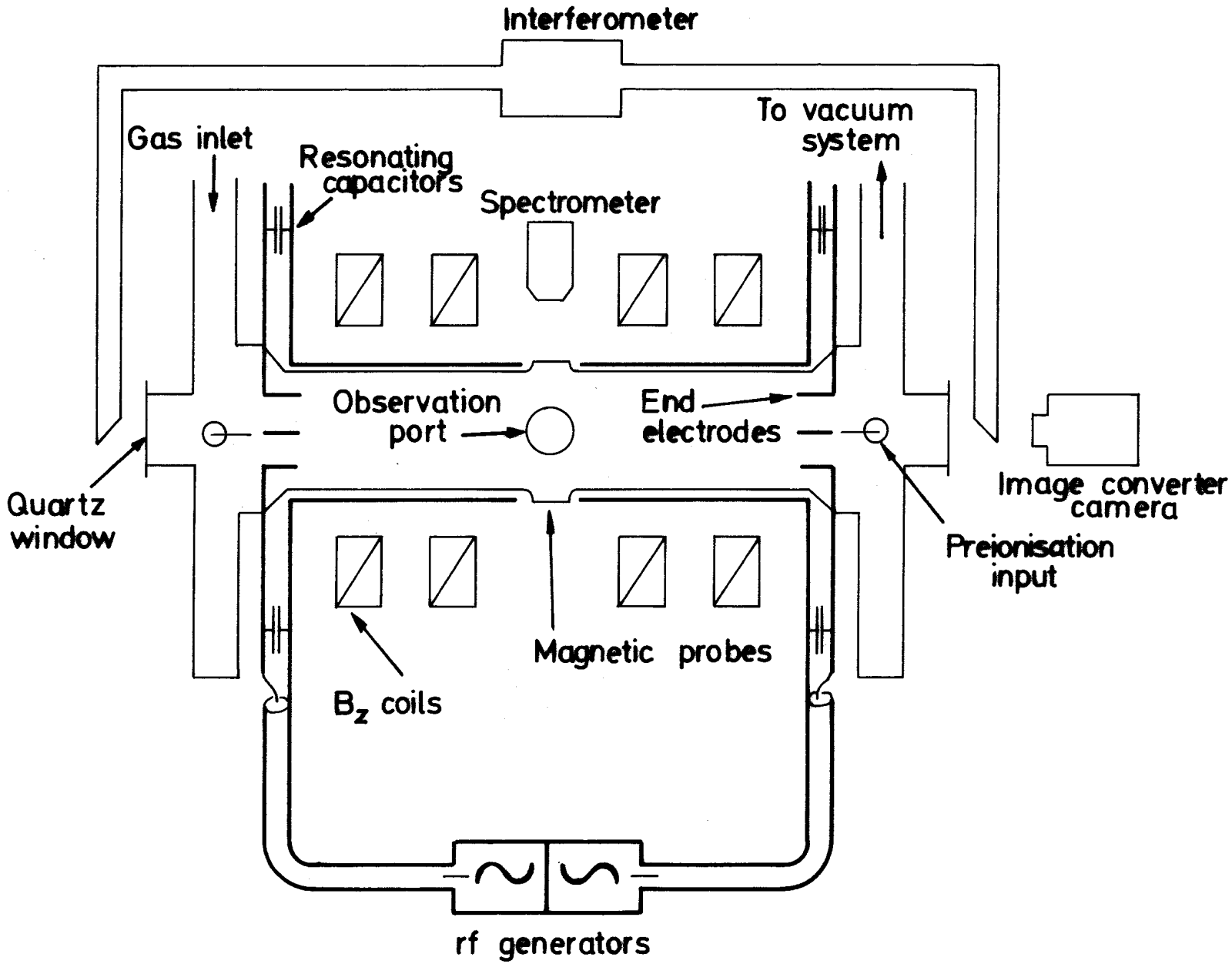
Interferometer
Gas inlet
Resonating capacitors
Spectrometer
To vacuum system
Observation port
End electrodes
Quartz window
Image converter camera
Preionisation input
Magnetic probes
B_z coils
rf generators

Fig.1

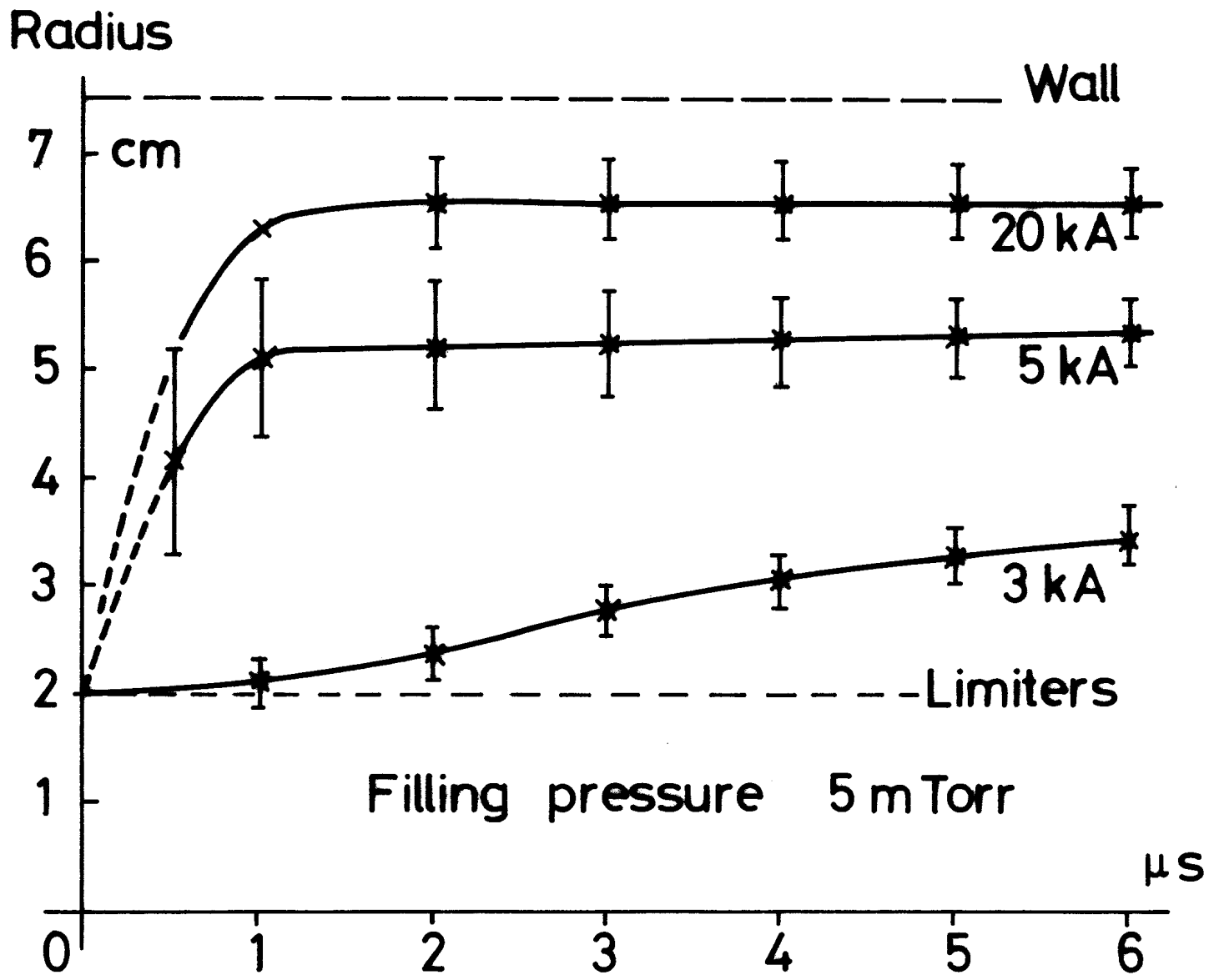
Radius
Wall
7
cm
6
5
4
3
2
1
20 kA
5 kA
3 kA
Limiters
Filling pressure 5 m Torr
μs
0
1
2
3
4
5
6

Fig.2

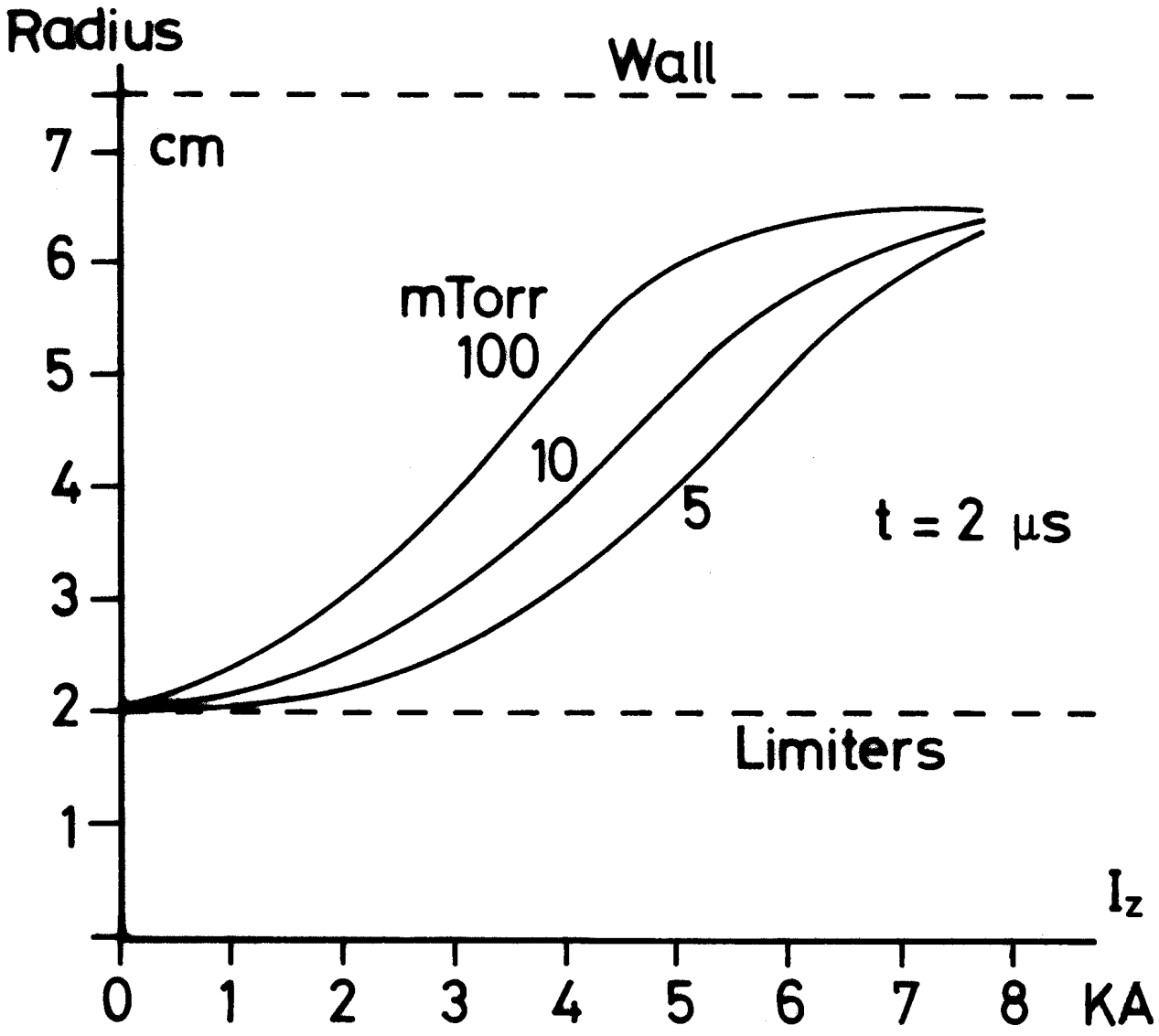
Radius
Wall
7
cm
6
mTorr
100
5
10
4
5
t = 2 μs
3
2
Limiters
1
I_z
0 1 2 3 4 5 6 7 8 KA

Fig. 3

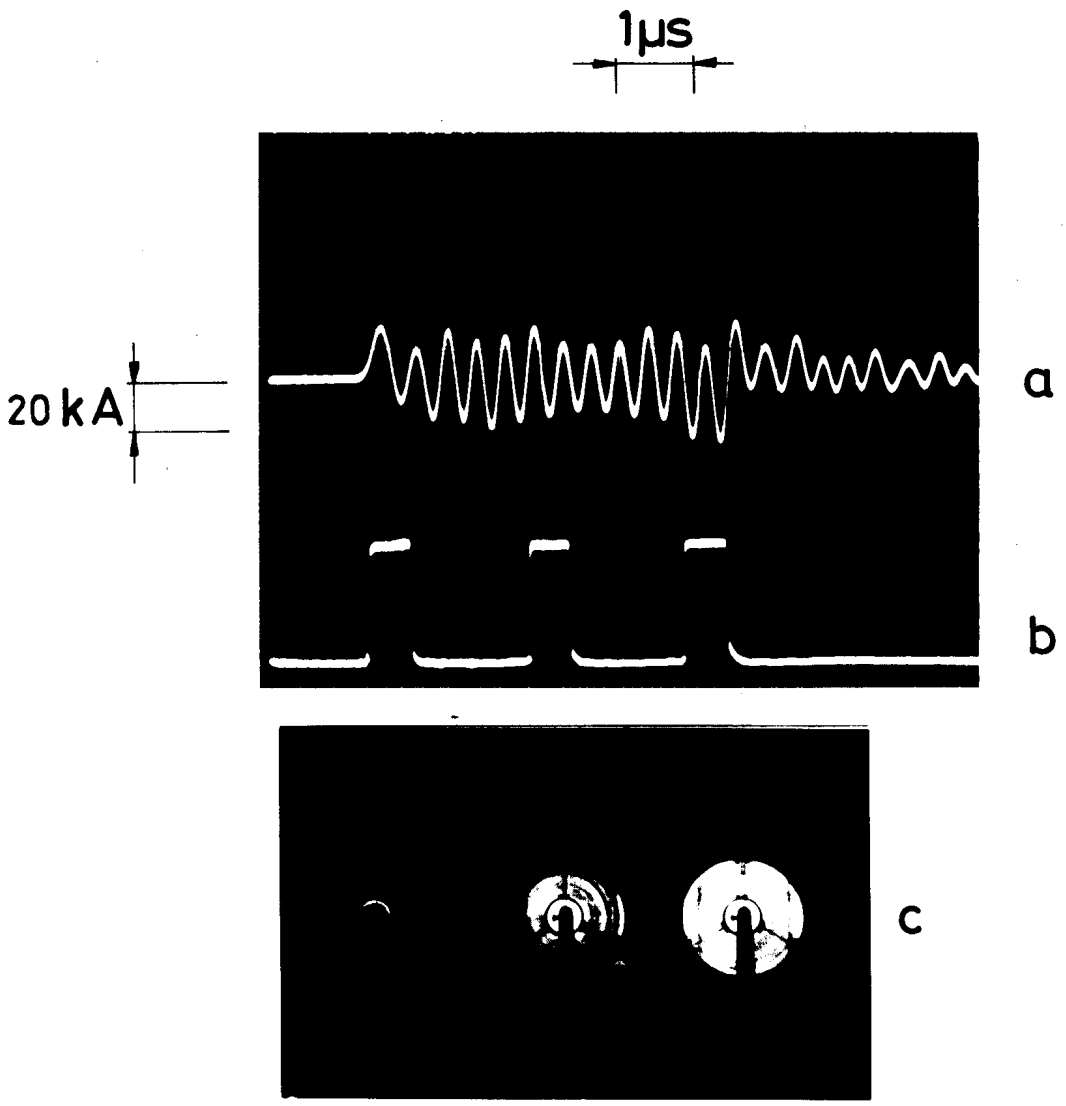

Fig 4

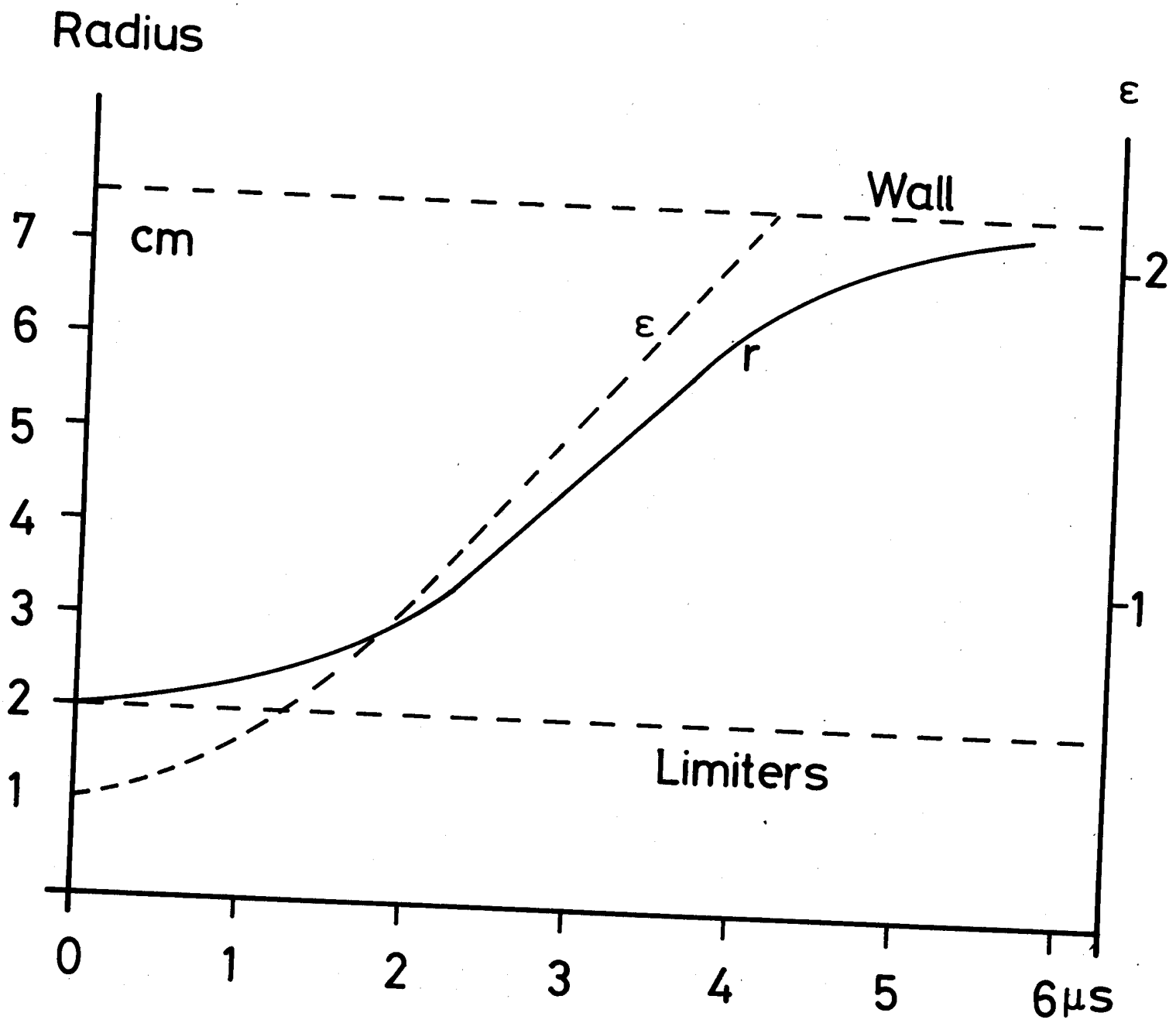

Fig 5

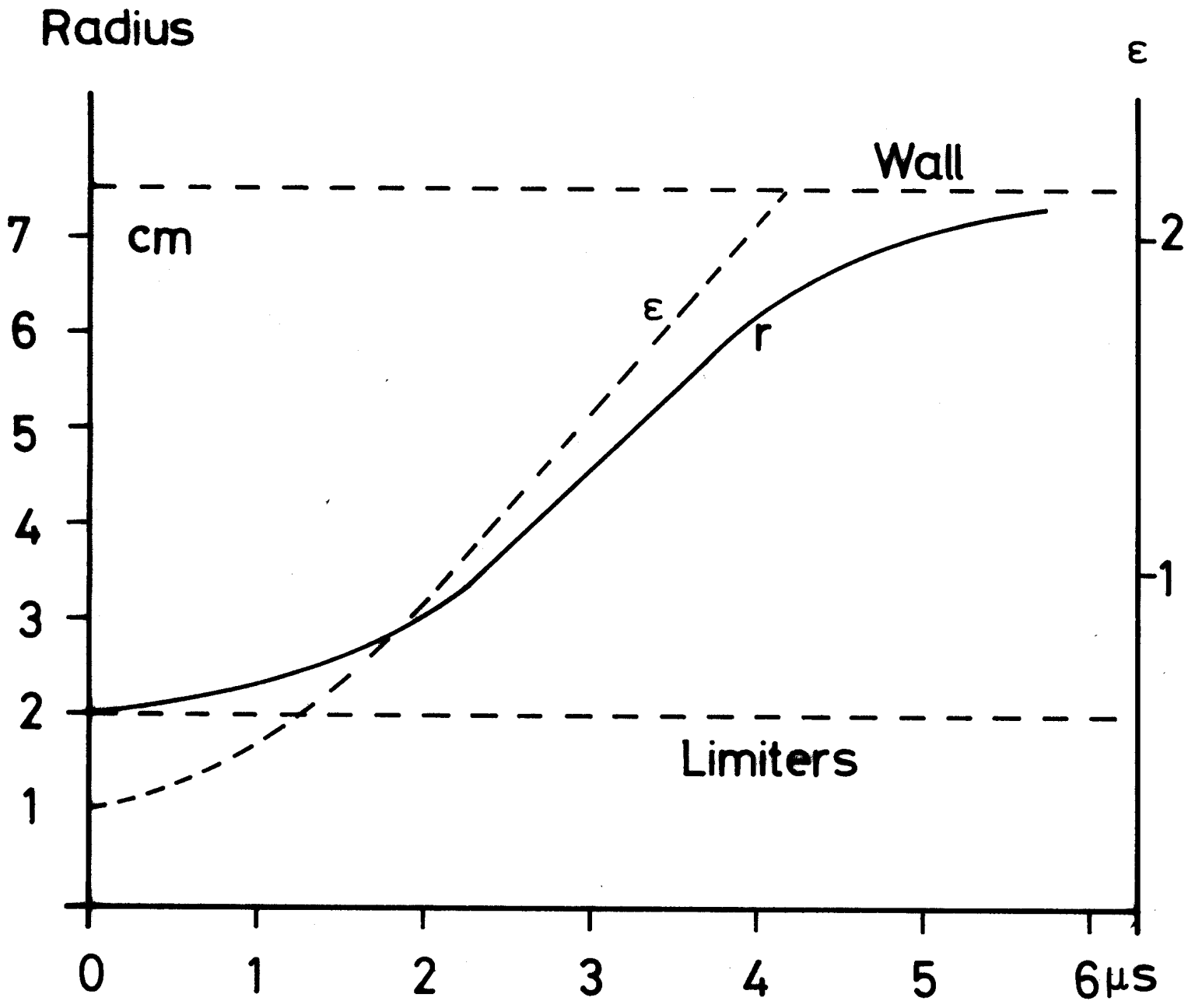

Fig. 6

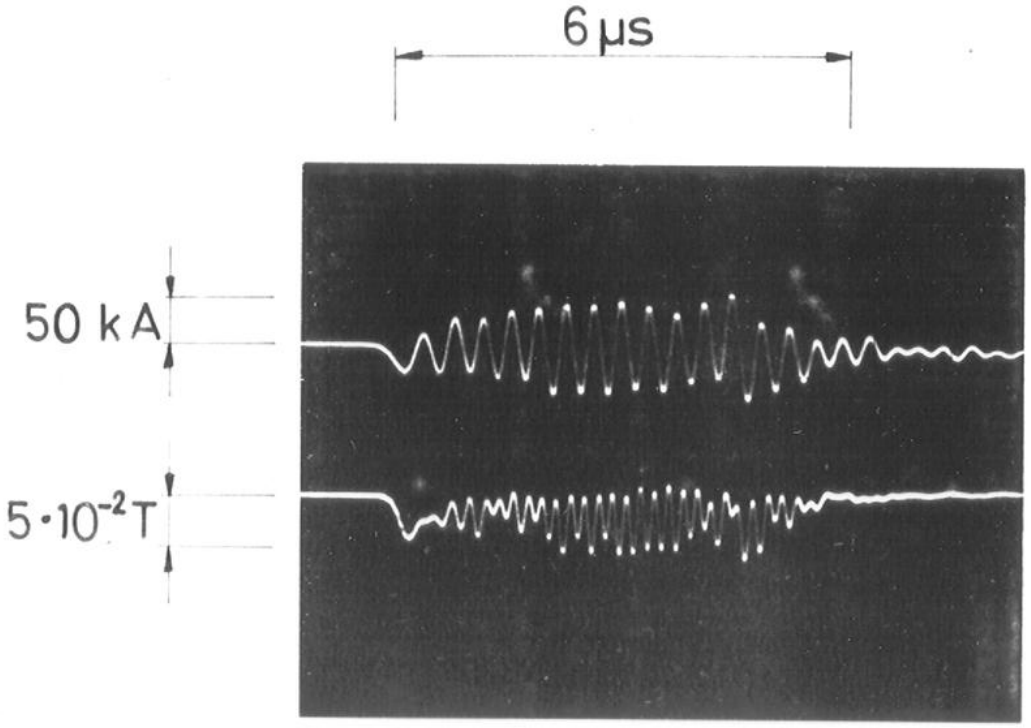
6 μs
50 kA
5·10⁻² T

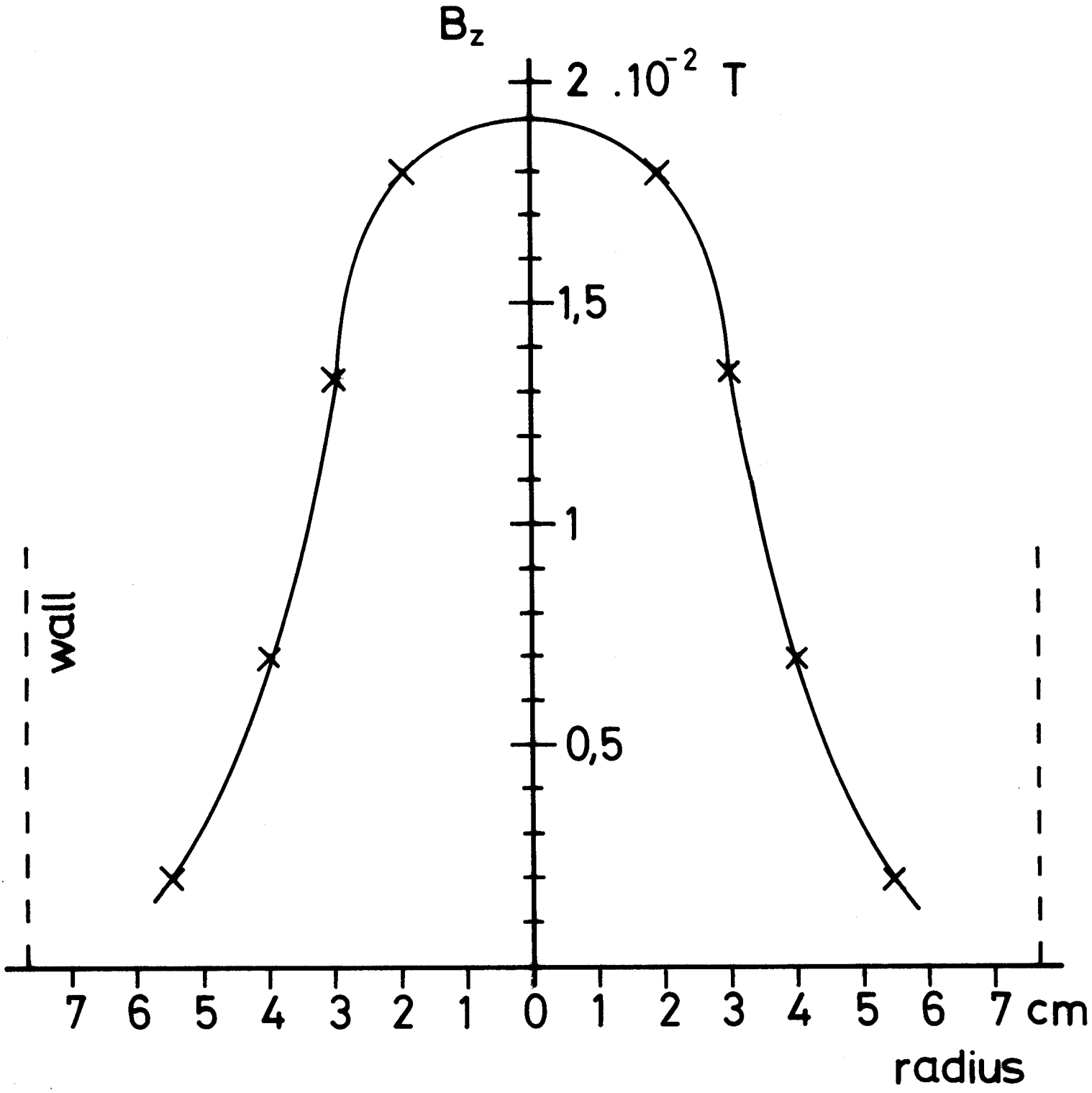

Fig. 8

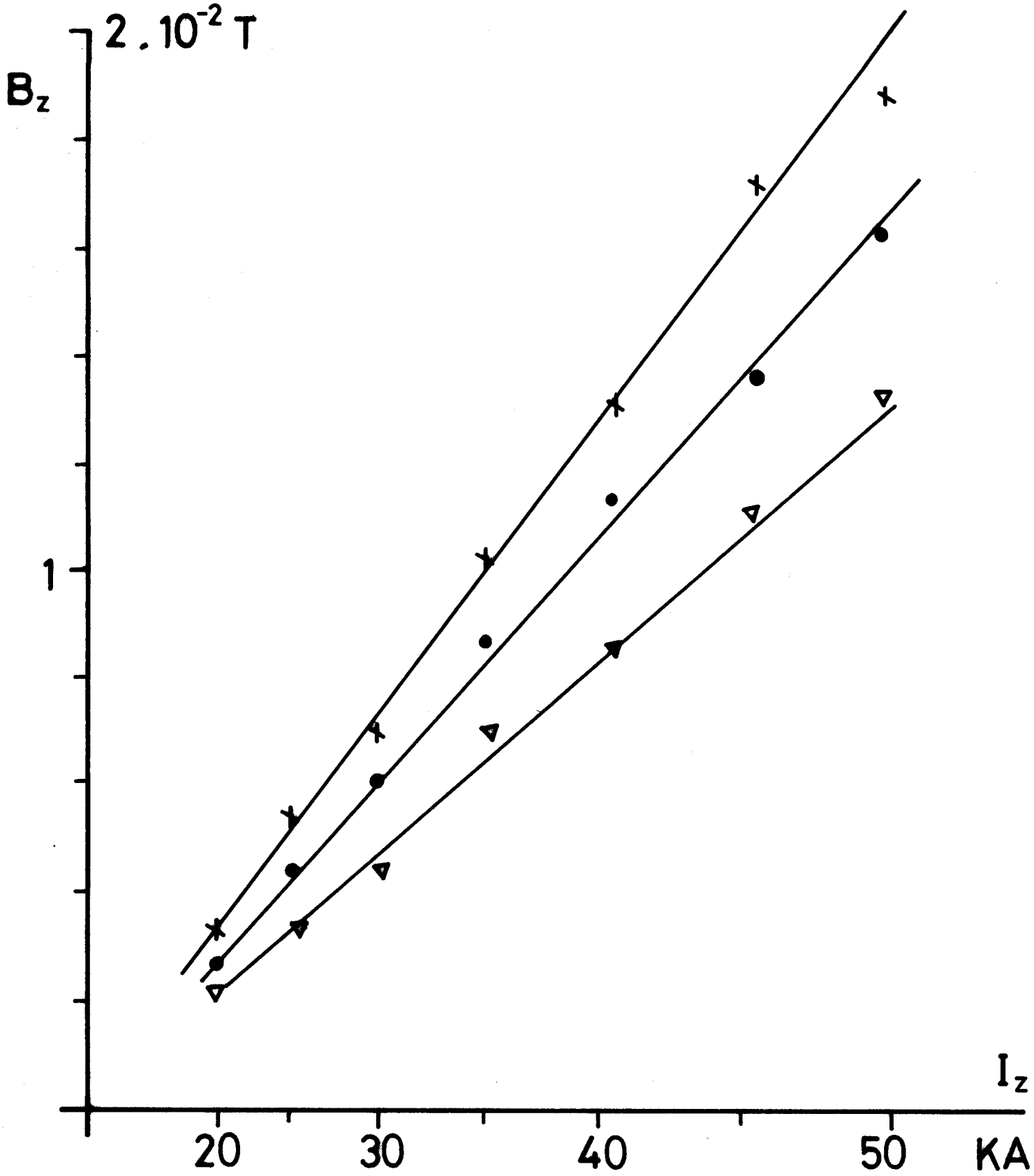

	n	B_o
×	$10^{20}\ m^{-3}$	0,40 T
●	$1{,}6 . 10^{20}$	0,45
▽	$3 . 10^{20}$	0,50

Fig.9

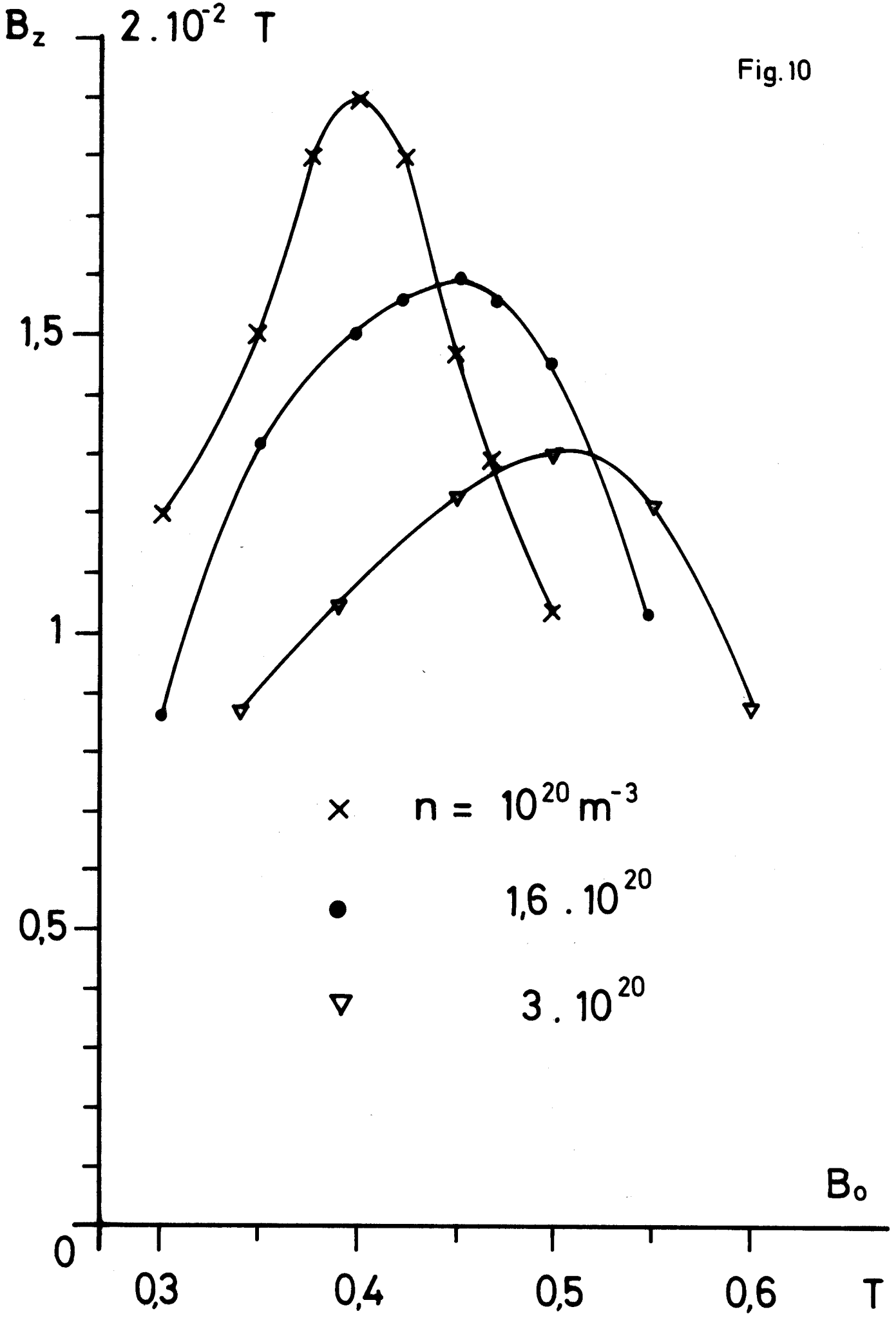

Fig. 10